

A monolithic evanescent field spore detector

D. A. Cohen, C. S. Wang, J. A. Nolde, D. D. Lofgreen, L. A. Coldren

Department of Electrical and Computer Engineering, University of California, Santa Barbara, CA 93106-9560
cohen@ece.ucsb.edu

Abstract: We demonstrate a monolithically integrated particle sensor based on evanescent field scattering, well suited for use with affinity assays for pathogen recognition. Single micron sized particles may be detected, representative of spores and small bacteria.

©2004 Optical Society of America

OCIS codes: (250.5300) Photonic integrated circuits; (140.5960) Semiconductor lasers

1. Introduction

Particle detection and identification is an important task in many industrial, pharmaceutical, medical, and security applications, and there is a growing need for particle sensors that are small, lightweight, fast, robust, and low enough in cost for widespread distribution. These requirements suggest that photonic integrated circuits may fill a significant market need. There have been many reports of integrated optic biochemical sensors achieving high sensitivity for both small and large molecules [1-3], but all required external light sources or optics which added significant size and manufacturing cost. We previously reported an optoelectronic sensor that included a monolithic laser to avoid this alignment task [4]. Those experiments all focused on the detection of molecular antigens captured on a waveguide surface by high affinity binding to antibodies or nucleotides, and careful control was needed to achieve sensitivity and stability. In contrast to molecular targets, there is an important class of pathogens that includes bacteria and bacterial spores, which range in size from one to ten microns in diameter. Cellular species have also been detected with miniature diode laser based instruments [5], but not previously with fully integrated devices. We report here the use of a simple monolithic particle sensor based on scattering of the evanescent field from a novel sensing waveguide. In conjunction with an appropriate affinity assay, the sensor may detect specific pathogens at the single cell level.

The sensor has been described previously, within the context of molecular sensing [6]. It consists of a gain section, a passive sensing region, and a waveguide photodetector all coupled by a single ridge waveguide, as shown in Fig. 1. A coupled cavity laser is formed between the cleaved facet at one end of the gain section, and the pair of etched facets bounding the passive section. The evanescent field of the optical mode penetrates slightly above the waveguide, and interacts with the sample fluid surrounding the waveguide. Optical scattering by particles bound to the waveguide surface increase both the cavity loss and reduce the light coupled to the waveguide photodetector, resulting in a reduction in photocurrent for a given laser bias current.

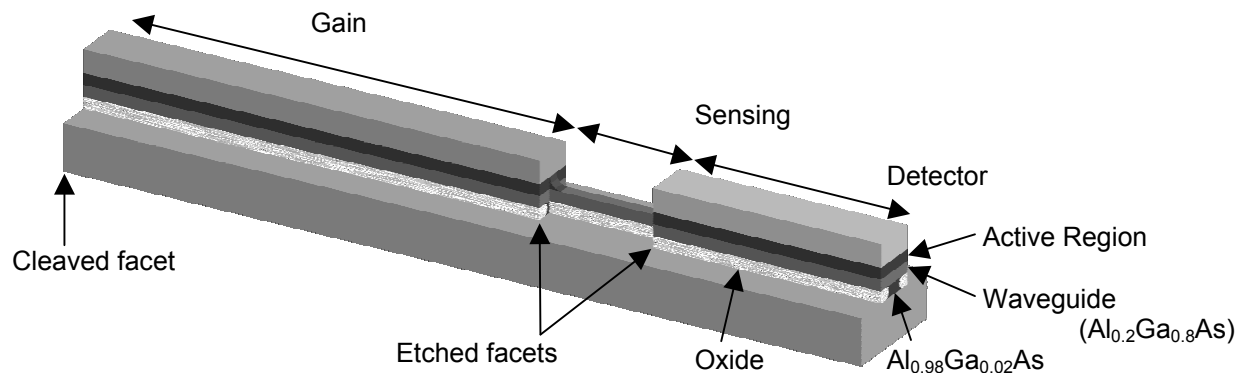


Fig. 1. Schematic of the coupled cavity laser sensor. Note the narrower ridge width in the sensing region, allowing complete oxidation beneath the waveguide layer to form a quasi-symmetrically clad waveguide.

It has been shown that for optimal sensitivity to thin chemical layers surface-bound to the sensing waveguide, as used, for example, in affinity assays, the sensing waveguide must be symmetrically clad, with a large index contrast between core and cladding [7]. Symmetrically clad dielectric waveguides have been demonstrated with very high sensitivity for bulk sensing, but due to the small index contrast, they offer only modest optical overlap with thin surface-bound layers. The need for careful alignment between the integrated laser's semiconductor waveguide and the dielectric waveguide also makes fabrication difficult. An all-semiconductor waveguide has also been demonstrated, but the highly asymmetric cladding limited the mode overlap with an analyte to 0.02% [4]. We developed a process for fabricating a self-aligned, semiconductor core, quasi-symmetric sensing waveguide monolithically-integrated with a conventional ridge laser. The resulting mode optical mode was tightly bound near the waveguide surface, with a 4.8% overlap with the analyte.

2. Fabrication

The major obstacle in constructing a symmetric waveguide was incorporating a low index material below the semiconductor core. This was accomplished without using a difficult regrowth or etching process, but rather by oxidizing a 300 nm $\text{Al}_{0.98}\text{Ga}_{0.02}\text{As}$ layer below the core. The laser itself employed an offset quantum well structure. The active region consisted of three 8 nm InGaAs wells with 8 nm GaAs barriers, grown above a 200 nm thick waveguide core composed of $\text{Al}_{0.2}\text{Ga}_{0.8}\text{As}$. Fabrication began by etching down to the waveguide in the middle region, thereby eliminating the absorbing quantum wells and forming a trench for the sensing region. Next, the ridge was patterned such that the middle region was narrower than the gain and absorber sections. Upon exposing the $\text{Al}_{0.98}\text{Ga}_{0.02}\text{As}$ after etching, a wet oxidation was performed to completely oxidize the sensing region in the middle but not completely oxidize under the gain and absorber sections. Thus, the effective widths of all three sections were nearly the same, 3 microns, providing a single lateral mode. The gain, sense, and absorber sections were 400, 40 and 200 microns long, respectively. The process was finalized with Ti/Pt/Au p-contacts, and AuGe/Ni/Au n-contacts on the back of the thinned substrate.

3. Results

To measure the mode overlap with an analyte, the shift in the optical spectrum due to changes in the analyte's index of refraction was measured, as described in [6]. The shift occurred because the passive cavity formed a Fabry Perot mode filter whose center wavelength depended on the refractive index of the medium surrounding the passive waveguide. The filter wavelength shifted nearly linearly with the index of refraction of the bathing fluid. To rule out errors due to temperature effects, the entire device was submerged in a temperature-controlled bath of fluid held at $18^\circ\text{C} \pm 0.1^\circ\text{C}$, and the gain section was biased with 500 ns pulses at a repetition rate of 10 kHz. From the data, the mode overlap with the fluid was calculated to be 4.8%, a hundred-fold improvement over previous work with an asymmetrically-clad waveguide, and in good agreement with 2D mode simulations.

We demonstrated a monolithic particle detector by reverse biasing the absorber section, and using it as an integrated photodetector. The gain section was biased at a fixed current, and the resulting photocurrent was monitored. A nanoliter drop of water containing about one thousand 1 micron diameter latex spheres was placed on the sensing region. The reflectivity at the etched facet between the gain and sensing regions was lowered by the presence of water, and so the laser's threshold current increased and the output power at fixed current decreased, as shown in Fig. 3. After 15 seconds, the water evaporated, and the signal increased again, but not quite to the original level. A photomicrograph of the sensing region revealed that a cluster of particles landed on the waveguide when the water evaporated, also shown in Fig. 3. Such a cluster is similar in size to a cluster of Anthrax spores. The sensitivity was high enough to detect single 1 μm latex particles.

4. Discussion

As with other sensors based on refractometry, for example surface plasmon resonance sensors or waveguide interferometers, this particle detector relies on selective binding chemistry to differentiate between target analytes and all other species. Thus, a useful device would also require a layer of ligand molecules deposited on the surface of the sensing waveguide, and a microfluidic means to deliver the sample and perhaps wash away contaminating particles. We note that the nearly instantaneous response of this sensor allows easy discrimination between discreet

particle binding events and slow changes due to an accumulation of serum proteins, a problem that has plagued other affinity sensors. Also, if the binding layer is restricted to the central two microns of waveguide width, where the field intensity is relatively uniform, then the magnitude of the response can also be used as a measure of the particle size, providing some additional discrimination against fouling by unsought particles.

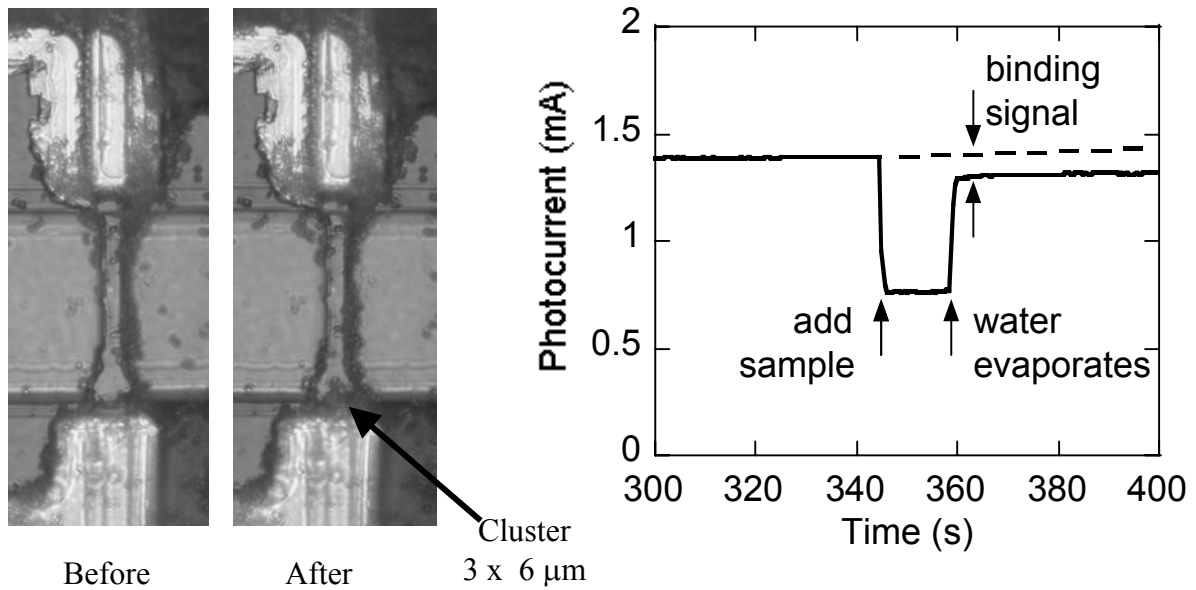


Fig. 3. Particle sensing with the coupled cavity laser sensor. A nanoliter droplet of water containing 1 micron diameter latex spheres is placed on the sensing waveguide and allowed to evaporate, leaving behind spheres or small clusters of spheres. The difference in photocurrent measured at the absorber indicates the presence of particles, seen in this case to be a single cluster similar in size to a cluster of anthrax spores.

5. References

- [1] R. G. Heidemann et al., "Remote opto-chemical sensing with extreme sensitivity: design, fabrication and performance of a pigtailed integrated optical phase-modulated Mach-Zehnder interferometer system," *Sensors and Actuators B*, **B61**, 100-127, (1999).
- [2] W. Lukosz, "Integrated optical chemical and direct biochemical sensors," *Sensors and Actuators B*, **B29**, 37-50, (1995).
- [3] C. F. R. Mateus et al., "Ultra sensitive optoelectronic label-free biosensor for static and dynamic monitoring of protein interactions," in *2003 LEOS Annual Meeting Conference Proceedings*, (Institute of Electrical and Electronics Engineers, New York, 2003), paper PD 2.4.
- [4] D. A. Cohen et al., "Monolithic chemical sensor using heterodyned sampled grating DBR lasers," *Electronics Letters*, **37**, 1358-1360, (2001).
- [5] P. L. Gourley et al., "Nanolaser/microfluidic biochip for realtime tumor pathology," *Biomedical Microdevices*, **2**, 111-122, (1999).
- [6] C. S. Wang et al., "A diode laser chemical sensor utilizing an oxidized lower cladding layer for high sensitivity," in *2003 LEOS Annual Meeting Conference Proceedings*, (Institute of Electrical and Electronics Engineers, New York, 2003), pp. 989-990.
- [7] O. Parriaux et al., "Normalized analysis for the sensitivity optimization of integrated optical evanescent-wave sensors," *IEEE J. Lightwave Technology*, **16**, 573-582, (1998).